LEO Dynamic Orbit Enhancement Using Atmospheric and Empirical Force Modeling

Tae-Suk Bae, *The Ohio State University*

BIOGRAPHY

Mr. Tae-Suk Bae is a Ph.D. candidate in the Department of Civil and Environmental Engineering and Geodetic Science, and a Graduate Research Associate in the Satellite Positioning and Inertial Navigation (SPIN) Laboratory at The Ohio State University. He received his M.S. and B.S. degrees in the field of surveying and photogrammetry from Seoul National University, Korea. His research interests cover GPS positioning algorithms, kinematic and dynamic orbit determination, gravity modeling, and spectral analysis in geodesy. Currently, he is working on algorithmic development and software implementation for the Low Earth Orbiters (LEOs) orbit determination with GPS.

ABSTRACT

In recent years, many Low Earth Orbiters (LEOs) have been launched for scientific purposes, such as Earth gravity recovery and atmospheric profiling for GPS meteorology, and new missions are expected in the next few years. CHAMP (CHAllenging Minisatellite Payload) is one of the recently (2000) launched missions designed for static Earth gravity field recovery, magnetic field mapping and atmospheric/ionospheric profiling. The CHAMP satellite has been placed in an almost circular, near polar orbit with an initial altitude of 450 km, and the mission is managed by GeoForschungsZentrum (GFZ). To meet the scientific mission objectives of LEOs, a precise orbit determination of the LEO satellites must be provided, although the required accuracy may be different for each application. LEOs, however, experience highly complex dynamics in their orbits due to the significant impact of high frequency gravity field components and atmospheric effects, which make it complicated to achieve an accurate orbit solution for a LEO.

Numerous efforts were undertaken to measure the nonconservative forces with the CHAMP onboard accelerometer data provided by GFZ (http://www.gfz-potsdam.de/pb1/op/champ/index_CHAMP.html). These data, however, do not represent all nonconservative forces properly. This is because the accelerometer data provided to the analysts are smoothed, based on a moving average of up to 10 data points. Therefore, the published accelerometer data are not sufficient for LEO Precise Orbit Determination (POD) since there might still be some dynamics between the consecutive epochs of data. Of all the nonconservative forces, the atmospheric drag is the most dominant in the LEO POD; therefore, its effect on the orbit solution is studied and presented in this study, based on the CHAMP satellite.

In this study, the parameters of the atmospheric drag are estimated on an hourly basis using two different atmospheric models, that is, NRLMSISE-00 and Jacchia 1971, and the results are compared to the solution obtained with a single drag coefficient estimated for the entire arc. It is shown that by estimating the nonconservative forces in the orbit determination (OD) process, the orbit can be substantially improved (compared to the case with no orbit improvement performed), resulting in ~13 cm 3D RMS (root mean square) error with respect to the Rapid Science Orbit (RSO) provided by GFZ. This orbit can be further improved up to 8 cm 3D RMS when the empirical force modeling is included. The software used in these analyses is the new OD software package developed by the author.

INTRODUCTION

The atmospheric effect on the geodetic mission satellite has been studied for a long time, since the high-altitude (5900 km) geodetic satellite LAGEOS (Rubincam, 1990) to the current gravity missions, such as CHAMP (König and Neumayer, 2003). Most of the geodetic mission satellites are usually deployed at 200 km to 1500 km altitudes, thus proper atmospheric modeling is very important for their mission objectives. The atmospheric drag forces and other nonconservative forces can either be modeled in the orbit determination process or can be theoretically replaced by the onboard STAR accelerometer data, as in the case of the CHAMP satellite.

Many atmospheric models were developed to accommodate its effect; however, it is difficult to cover all the details of the atmospheric effects for the LEO missions, because LEO satellites have irregular shapes and their surface materials demonstrate complex properties. Atmospheric density, in general, varies with the solar flux and geomagnetic activity index (Montenbruck and Gill, 2001), and also depends on the time and the Sun-to-satellite path. The onboard accelerometer data of CHAMP can measure all nonconservative forces in three directions (Kang et al., 2003); however, one is required to estimate the bias and the drift of the accelerometer sensors. Even if the bias and drift are estimated, the total replacement of the nonconservative forces with the accelerometer data is not possible because the published accelerometer data are smoothed over a 10-second interval, while there still could be more dynamics or maneuvers during the smoothing interval (H. Boomkamp, 2004, personal communications). Therefore, the nonconservative forces, which are dominated by atmospheric drag forces, must be modeled and improved in the orbit determination process.

The accurate and careful modeling of atmospheric drag is particularly important during geomagnetically disturbed intervals. During magnetic storms, the atmospheric density increases due to deposition of energy by particles precipitating from the magnetosphere, and by ohmic heating of ionospheric currents driven by ionosphere-magnetosphere coupling. The precipitating particles also ionize the upper atmosphere, which increases the conductivity and, ultimately, the ohmic heating. The increased atmospheric densities, with possible significant spatial and temporal variation, lead to increased satellite drag (deceleration), which must be properly accounted for in the orbit determination procedure.

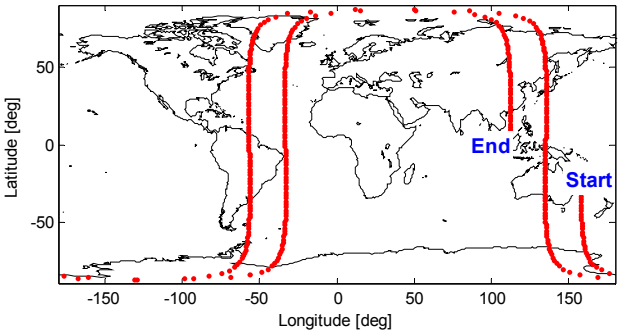

Figure 1: The trajectory of CHAMP (15 Feb. 2003, 2:00-5:00)

In general, the atmospheric density can be modeled from spectrometer measurements or satellite orbit dynamics. Since the atmospheric models are undersampled at geodetic satellite altitudes (> 750 km) and during high solar and/or geomagnetic activity they are extrapolated, the scaling factors for the atmospheric drag are generally estimated for precise orbit determination (http://www.agu.org/revgeophys/marsha01/node13.html).

In this study, two different atmospheric models, that is, NRLMSISE-00 and Jacchia 1971, are used and their effects are compared in terms of the final estimated dynamic orbit error. In addition, the empirical forces, which can replace the remaining (unmodeled) orbital errors, are also discussed, since the drag forces and the empirical forces are the most dominant among the nonconservative forces, while modeling of the other nonconservative forces are straightforward. Two revolutions of the CHAMP orbit on 15 Feb. 2003 are used to test the validity of the modeling (Figure 1).

DYNAMIC ORBIT DETERMINATION

Most orbit determination procedures are designed as dynamic, because the kinematic orbit determination method depends entirely on the observational geometry and GPS signal continuity; thus a purely kinematic solution might not always be of sufficient quality and continuity due to insufficient observations and poor geometric configuration (Byun, 2003). In the dynamic approach, all the forces acting on the satellite orbits are computed and integrated numerically to estimate the initial state vectors (position and velocity) and other unknown force parameters (Grejner-Brzezinska, 1995; Bock, 2003). The position and the velocity of a LEO satellite in the following epochs can then be propagated from the initial states using the force models. Therefore, accurate force models are mandatory for dynamic orbit determination. Since the current LEO missions (e.g., CHAMP, GRACE) carry space-grade GPS receivers onboard, the measurements to the GPS satellites are used as observables, which are connected to the unknown force parameters of the LEO via the variational partials to improve the final orbit solution. Due to the nonlinear relationship between the observed quantities and the unknown parameters, the parameter estimation is usually accomplished by a batch least-squares method in the iterative mode.

In this study, the triple-differenced ion-free carrier phase linear combinations are used as primary observables in the orbit determination software package developed by the author. The triple-differenced GPS observables were successfully applied for both the dynamic GPS satellite orbit determination process and the LEO kinematic OD (see, for example, Grejner-Brzezinska, 1995; Bae et al., 2002; Kwon et al., 2003; Byun, 2003; Bock 2003). In the triple-differencing technique, the integer ambiguity parameters as well as the receiver and satellite clock errors are removed through satellite-to-satellite and time differencing of the observables (Hofmann-Wellenhof et

al., 1997). In addition, there is no need to detect and correct the cycle slips, which are simply treated as data outliers, *i.e.*, large residuals. However, in general, triple-differencing amplifies the noise of the observables and introduces a correlation between epochs by sharing a common epoch. The nondiagonal variance-covariance matrix can, however, be easily handled with an efficient algorithmic approach, such as Cholesky decomposition (Grejner-Brzezinska, 1995). All in all, triple differences, combined with efficient matrix manipulation techniques, provide fast, accurate and effective OD solution.

The triple-differencing technique was first applied to GPS dynamic orbit determination by Grejner-Brzezinska (1995). Since GPS orbits are at a very high altitude, the orbits are much smoother as compared to a LEO. In the LEO case, however, the usual altitude is about 450-700 km, there should be much more perturbation coming from geopotential, atmospheric drag, etc.; moreover, the complicated shape of the spacecraft makes the force modeling (and thus, the OD process) more difficult.

Let $\mathbf{r}_{3\times1} = [x \quad y \quad z]^T$ be the vector of satellite position coordinates of the LEO at each epoch. The general form of the equations of motion of the satellite in the Earth-centered inertial frame is given as follows (Hugentobler et al., 2001):

$$\ddot{\mathbf{r}} = -\frac{GM}{r^3}\mathbf{r} + \mathbf{a}(t, \mathbf{r}, \dot{\mathbf{r}}, \mathbf{p}) \tag{1}$$

where:

- $\ddot{\mathbf{r}}$: the total acceleration of the satellite at time t,
- GM : the product of the gravitational constant and the mass of the Earth,
- r : the magnitude of the position vector $\mathbf{r}$,
- $\mathbf{a}$: the total perturbing forces,
- t : time, at which the acceleration is calculated,
- $\dot{\mathbf{r}}$: the velocity of the satellite at time t,
- $\mathbf{p}$: the parameter vector, which induces the perturbing acceleration.

The parameter vector $\mathbf{p}$ includes the nonspherical part of the Earth's gravity field, the luni-solar and planetary gravitational attraction, atmospheric drag, solar radiation pressure and/or some empirical force terms, which normally account for all unmodeled force terms. The magnitudes of the forces acting at approximated CHAMP altitude are given in Table 1.

As can be seen in Table 1, the atmospheric drag, which amounts to approximately 1000 m of error after two revolutions, gives a significant acceleration to the LEO, as compared to other perturbing forces. Note that the values in Table 1 represent the average of each value for two revolutions.

Table **1**: The magnitude of the forces acting on the LEO at CHAMP altitude.

Forces	Magnitude [m/s^2]
Keplerian term	8.66
J_2	1.6×10^{-2}
Nonspherical gravity field	2.1×10^{-4}
Sun/Moon	1.3×10^{-6}
Atmospheric drag	5.3×10^{-7}
Empirical force	3.4×10^{-7}
Relativistic effect	2.1×10^{-8}
Solar radiation pressure	7.6×10^{-9}

ATMOSPHERIC MODELS

As mentioned earlier, since the atmospheric effect is significant at the LEO altitude, the acceleration due to atmospheric drag must be properly evaluated in the LEO OD process. It is difficult, however, to model the atmosphere accurately because the physical properties of the atmosphere (the density of the upper atmosphere) are not sufficiently known; moreover, a detailed knowledge of the interaction of neutral gases as well as charged particles with the different spacecraft surfaces is required. In addition, the varying attitude of nonspherical satellites with respect to the atmospheric particle flux makes its modeling even more difficult (Montenbruck and Gill, 2001). Numerous atmospheric models have been published and are currently in use; the two commonly used models, Jacchia 1971 and NRLMSISE-00, are analyzed here.

JACCHIA 1971 MODEL (J71)

The J71 model is a function of the geodetic height, temperature and time, which represents the spatial and temporal parameters needed to estimate the accelerations due to drag at the satellite location at a given epoch. The J71 model assumes the following: 1) the chemical constituents of the atmosphere are in a state of mixing below 100 km, and 2) the atmosphere is in diffusion equilibrium at higher altitudes. The steps to compute the atmospheric density in J71 model are given as follows (Montenbruck and Gill, 2001):

1) compute the exospheric temperature T_∞ from the solar activity and geomagnetic index,
2) compute the standard density using a bi-polynomial fit with the altitude and the exospheric temperature parameters, and
3) apply the time-dependent corrections to get the atmospheric density at given time and location.

The time-dependent corrections in step 3) include the geomagnetic term, the semiannual density variation in the

thermosphere, and the seasonal-latitudinal effects. The effective altitude for this model ranges from 90 km to 2500 km. For detailed formulae, see Montenbruck and Gill (2001, pp. 91-98).

NRLMSISE-00 MODEL

The NRL Mass Spectrometer, Incoherent Scatter Radar Extended Model (NRLMSISE-00) was developed, based on satellite mass spectrometer and ground-based incoherent scatter data, to provide a single analytic model for calculating temperature and density profiles (Hedin, 1991; MSIS, 2004). This model is a function of many different variables, *i.e.*, local time, latitude, annual/semiannual, and longitude variations. It is expanded in terms of the lower-order spherical harmonics and the Fourier series with the parameters of the temperature profile and density boundary conditions at 120 km. This model allows for easy determination of temperature and density profiles for specific geographic and solar/magnetic parameters.

The official release of the FORTRAN code for the NRLMSISE-00 atmospheric model can be found at http://uap-www.nrl.navy.mil/models_web/msis/NRL_MSISE-00.DIST17.TXT. This subroutine requires time, location, solar radio flux at 10.7 cm in units of 10^{-22} W/(m^{2}Hz) and the magnetic activity index as input variables, and provides the atmospheric densities as well as total mass density and temperature at the desired altitude. The actual solar flux and the magnetic index data and their formats can be found at ftp://ftp.ngdc.noaa.gov/STP/GEOMAGNETIC_DATA/INDICES/KP_AP/.

Figure 2 represents the total mass density variation of the two models along the trajectory tested in this study. The models are relatively close to each other, except for a few discontinuities on the J71 model around 2:15 and 3:45.

THE ATMOSPHERIC FORCE MODELING

As can be seen in Table 1, the atmospheric drag is the most significant nonconservative force, especially for the LEO altitude. In order to model the atmospheric drag, the well-known equation

$$\ddot{\mathbf{r}} = -\frac{1}{2} C_D \frac{A}{m} \rho v_r^2 \mathbf{e}_v , \tag{2}$$

can be used (Montenbruck and Gill, 2001), where m is the spacecraft mass, the drag coefficient C_D is a dimensionless quantity that describes the interaction of the atmosphere with the satellite's surface material (which

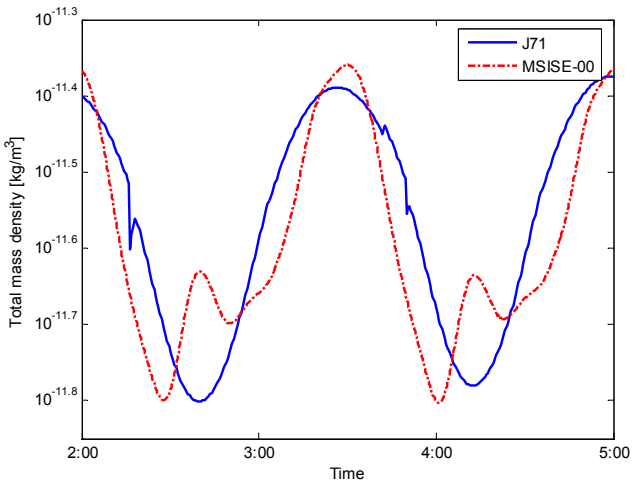

Figure 2: Total mass density along the CHAMP trajectory.

should be estimated in the OD process, as mentioned earlier), ρ is the density of the atmosphere at the location of the satellite, A is the area of the satellite surface perpendicular to the satellite velocity, and $\mathbf{v}_r$ is the velocity of the object relative to the atmosphere, which is given by Eq. (3)

$$\mathbf{v}_r = \mathbf{v} - \boldsymbol{\omega} \times \mathbf{r} , \tag{3}$$

$$\mathbf{e}_v = \frac{\mathbf{v}_r}{|\mathbf{v}_r|}, \quad v_r = |\mathbf{v}_r| \tag{4}$$

with the velocity vector $\mathbf{v}$ and the position vector $\mathbf{r}$ of the satellite in the inertial frame, and the Earth angular velocity vector $\boldsymbol{\omega}$ is as follows:

$$\boldsymbol{\omega} = [0 \quad 0 \quad \omega_e]^T \tag{5}$$

with the nominal value of $\omega_e = 7.292115486 \times 10^{-5}$ rad/sec.

The partial derivatives of the acceleration with respect to the drag coefficient, C_D, can be computed as shown in Eq. (6):

$$\frac{\partial \ddot{\mathbf{r}}}{\partial C_D} = \frac{\partial \ddot{\mathbf{r}}}{\partial C_D} + \frac{\partial \ddot{\mathbf{r}}}{\partial \mathbf{r}} \frac{\partial \mathbf{r}}{\partial C_D} . \tag{6}$$

The first term on the right side of Eq. (6) represents the explicit component of the partial derivatives, which can be easily computed from Eq. (2). The second term, however, is an implicit part of the partial derivatives, which require more careful attention. The partial derivatives of the position vector with respect to the drag coefficient can be obtained by numerical integration of Eq. (6) up to the current epoch. The partial derivative of the acceleration with respect to the position vector can be derived analytically as follows:

$$\frac{\partial \ddot{\mathbf{r}}}{\partial \mathbf{r}} = -\frac{1}{2} C_D \frac{A}{m} v_r^2 \mathbf{e}_v \frac{\partial \rho}{\partial \mathbf{r}} + \frac{1}{2} C_D \frac{A}{m} \rho v_r \left(\mathbf{e}_v \mathbf{e}_v^T + \mathbf{I}_3 \right) [\boldsymbol{\omega} \times], \quad (7)$$

where $\mathbf{I}_3$ represents the 3×3 identity matrix and from Eq. (5)

$$[\boldsymbol{\omega} \times] = \begin{bmatrix} 0 & -\omega_e & 0 \\ \omega_e & 0 & 0 \\ 0 & 0 & 0 \end{bmatrix}. \quad (8)$$

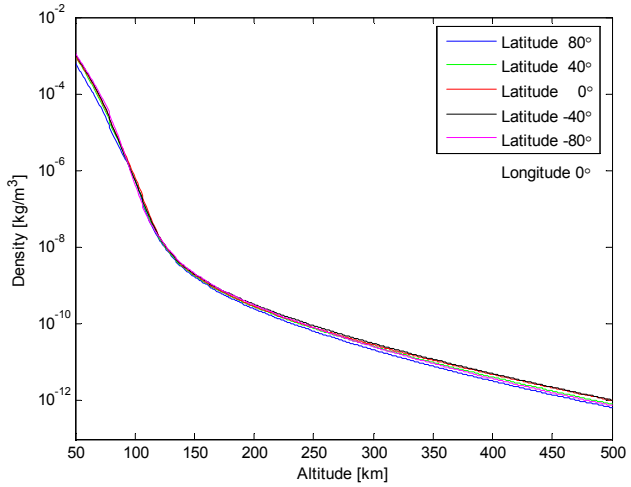

Figure 3: Density variation with altitude for different latitudes (NRLMSISE-00).

It should be mentioned that the partial derivative of the density with respect to the position vector cannot be easily computed analytically. As explained earlier, the atmospheric density models are very complex, thus difficult to express as simple analytic functions. Therefore, this partial derivative should be computed by numerical differentiation (Montenbruck and Gill, 2001). Test results (not shown in this paper) indicate that the numerical differentiation of the density for different positional variations makes only an insignificant difference (submillimeter level), because the density is a small value, as compared to the position vector (see the ratio $\partial \rho / \partial \mathbf{r}$ in Eq. (7)), and changes very smoothly; thus it is not so sensitive to the position changes (Figure 3).

THE EMPIRICAL FORCE MODELING

While including the atmospheric modeling and estimation in the OD process can considerably reduce the orbital errors, there still remain significant values of unmodeled forces (in practice, there is no model that covers 100 percent of a phenomenon that it represents). Therefore, a number of empirical harmonics can be used to absorb the variability of the nonconservative forces. Another approach is to estimate the pseudo-stochastic parameters, which represent the frequent, instantaneous velocity changes; however, the empirical force modeling can also absorb the high-frequency effects, such as thrusters firing, during the orbit determination process. Since the radial direction is dynamically coupled with the along-track direction, it is not explicitly modeled in the orbit determination process to avoid the ill-conditioning of the system (O. Colombo, 2002, H. Boomkamp, 2004; personal communications). Therefore, only the along-track and cross-track once-per-revolution components are estimated together with other parameters. The constant bias and the twice-per-revolution terms can also be modeled, depending on the type of satellite considered.

The periodic properties of the nonconservative (predominantly once-per-revolution and twice-per-revolution) forces can be clearly seen in Figures 4 and 5. Thus, the empirical force model can be expressed as a sum of sine and cosine terms in each direction:

$$\begin{aligned} \ddot{r}_{along} &= C_a \cos(u) + S_a \sin(u), \\ \ddot{r}_{cross} &= C_c \cos(u) + S_c \sin(u), \end{aligned} \quad (9)$$

where

C_a, S_a, C_c, S_c : the coefficients of sine and cosine in each direction,

u : the argument of latitude of the satellite.

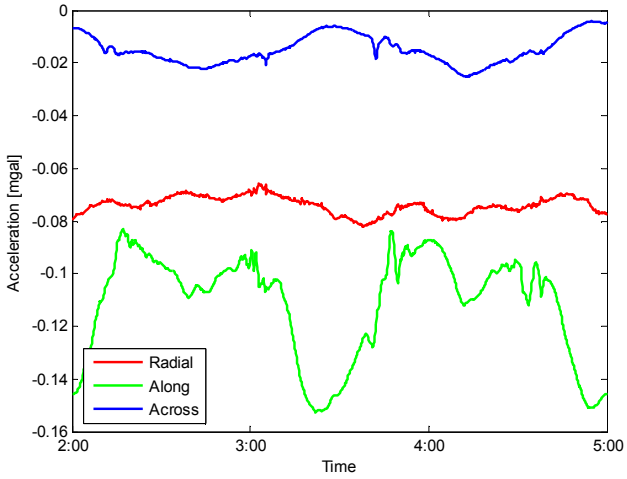

Figure 4: STAR accelerometer data for CHAMP representing nonconservative forces acting on the satellite.

Since the empirical forces are modeled in the RTN (Radial/Transverse/Normal) frame, these should be transformed into an inertial frame to be combined with other accelerations. This transformation matrix can be computed using the satellite inertial position and velocity, which is given as follows:

$$\ddot{\mathbf{r}}_{inertial} = \begin{bmatrix} \ddot{x} \\ \ddot{y} \\ \ddot{z} \end{bmatrix} = \begin{bmatrix} N_1 & T_1 & R_1 \\ N_2 & T_2 & R_2 \\ N_3 & T_3 & R_3 \end{bmatrix} \begin{bmatrix} \ddot{r}_{cross} \\ \ddot{r}_{along} \\ 0 \end{bmatrix}, \quad (10)$$

where

$$\mathbf{R} = [R_1 \quad R_2 \quad R_3]^T = \mathbf{r}/|\mathbf{r}|,$$

$$\mathbf{N} = [N_1 \quad N_2 \quad N_3]^T = \mathbf{v} \times \mathbf{R},$$

$$\mathbf{T} = [T_1 \quad T_2 \quad T_3]^T = \mathbf{R} \times \mathbf{N}$$

with the position vector $\mathbf{r}$ and the velocity vector $\mathbf{v}$ of the satellite in an inertial frame.

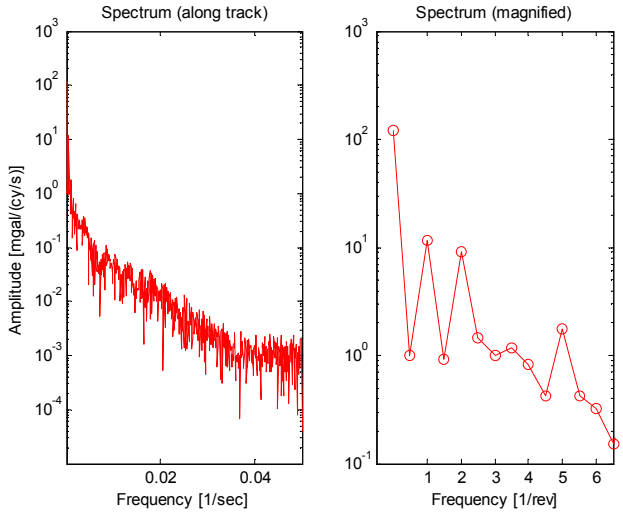

Figure 5: Fourier spectrum of STAR accelerometer data for CHAMP (along track).

TEST DATA

In order to test the orbit improvement due to the atmospheric and empirical force modeling, three hours of CHAMP data on 15 Feb. 2003, 2:00-5:00 (GPS time scale), which correspond to two full revolutions, are used in this study. The estimated parameters in the dynamic orbit determination (called the "reference case") are as follows:

- The initial state vector of CHAMP (position and velocity),
- The atmospheric drag coefficients (one parameter/arc),
- The solar radiation scale factor (one parameter/arc),
- The empirical force coefficients (once/revolution, twice/revolution).

The uncertainties of the initial position and velocity are assigned at 1 m and 0.1 m/s levels, respectively. They are added to the Rapid Science Orbit (RSO) published by GFZ, and selected for the zero epoch of the analyzed time interval, to get the approximation for the initial state vector. The NRLMSISE-00 model is used for the estimation of the atmospheric drag coefficients, and the area-to-mass ratio for CHAMP is given as 0.00138 m^2/kg (http://op.gfz-potsdam.de/champ/systems/index_SYSTEMS.html). The elevation cutoff angle of the GPS satellites is set to 10 degrees for the LEO and 15 degrees for 43 IGS ground stations used in this study; a 30-second sampling interval of GPS data was used for both CHAMP and IGS stations. The numerical orbit integration is also performed at the 30-second step. It should be mentioned that the simple cannon ball model is used for the atmospheric and solar radiation pressure modeling to represent the satellite's body. Also, data cleaning is performed during the estimation process by the residual criterion, as mentioned earlier.

TEST RESULTS

Figure 6 shows the resulting errors of the estimated orbit with respect to the RSO in the RTN frame, where the analyzed solution includes the atmospheric drag coefficient estimated every hour; the statistics for each of the one-hour arcs are presented in Table 2. The initial state uncertainty is estimated within 11 cm or less compared to RSO, and the overall RMS error for the two revolutions is about 8.5 cm. In general, there is always a larger error at both ends of the estimated arc due to insufficient data. Therefore, if we consider the middle section 2 only, the 3D RMS with respect to the RSO is only about 4 cm. Unfortunately, the test data is too short to draw a conclusion for a more generic case.

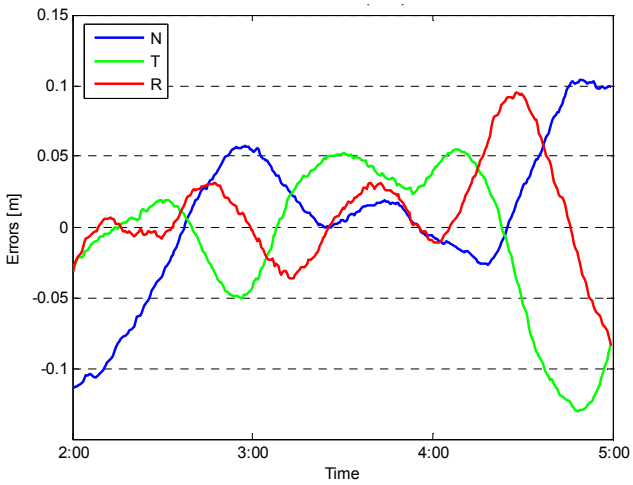

Figure 6: Orbit errors in RTN frame: RSO minus the solution with C_D estimated every hour.

Table **2**: Orbit errors w.r.t. the RSO in the RTN frame (unit: cm).

		Section			Entire arc
		1	2	3	
N	Mean	-2.91	1.58	3.46	0.71
	Std.	5.95	1.57	5.03	5.30
T	Mean	-1.01	2.79	-4.02	-0.75
	Std.	2.21	2.42	7.14	5.32
R	Mean	0.56	-0.06	2.39	0.96
	Std.	1.46	2.16	5.13	3.47

Table 3 represents the estimated unitless atmospheric drag coefficients for each section of one-hour arc. The coefficients can be different from each other by up to 25 percent for each section, indicating that atmospheric variability can be significant and thus, should be properly taken into account.

Table **3**: Estimated atmospheric drag coefficients (unitless).

Section	1	2	3
C_d	4.0285	4.9953	4.6132

The effect of the two atmospheric models used is tested for the "reference case" solution (*i.e.*, one atmospheric drag coefficient is estimated for the entire arc). According to Table 4, the resulting difference in 3D RMS is only about 0.5 cm, which seems insignificant if the drag coefficients are estimated in the OD procedure. However, it should be mentioned that the effect of each atmospheric model shown in Table 4 is different for each component N, T and R.

Table **4**: Mean and standard deviation of the orbit differences between the RSO and two solutions with different atmospheric models used (unit: cm).

		N	T	R	3D
NRLMSISE-00	Mean	0.89	1.50	-0.84	
	Std.	5.27	3.38	5.63	8.42
J71	Mean	1.01	0.64	0.95	
	Std.	6.99	4.48	3.18	8.89

Figure 7 shows the orbit difference for different numbers of estimated drag coefficients (one/arc vs. one/hour) in the RTN frame. It should be noticed here that if only the central part of the orbit is considered, *i.e.*, by excluding both ends of the orbit solution which has larger errors, the difference between the two cases is less than 0.8 cm in RMS for each component (Table 5).

Table **5**: Orbit comparison for solutions with different number of drag coefficients estimated (unit: cm).

		Section			Entire section
		1	2	3	
N	Mean	0.18	0.27	0.10	0.18
	Std.	0.07	0.13	0.10	0.13
T	Mean	0.82	0.31	0.80	0.64
	Std.	0.86	0.37	0.92	0.83
R	Mean	1.10	0.48	1.16	0.91
	Std.	1.16	0.57	1.11	1.10

Note: The "absolute average" is used for the mean value.

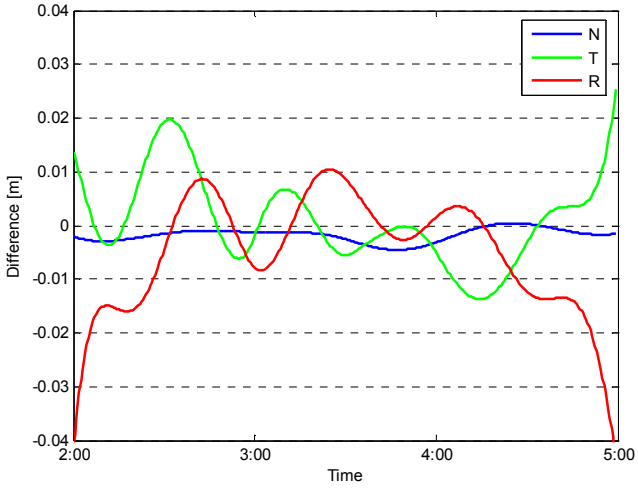

Figure 7: Orbit difference between solutions with different number of drag coefficients estimated (one/arc vs. one/hour).

SUMMARY AND CONCLUSIONS

The effect of the nonconservative forces on the LEO dynamic orbit is significant, as discussed in this paper. Among these forces, the atmospheric drag is the most dominant error source and should be dealt with with care in the orbit determination process. Two different atmospheric models, (*i.e.* NRLMSISE-00 and J71) were tested. The results indicate that the model choice does not make any significant difference if we estimate the drag coefficients, although they show slightly different error behavior for each orbital component.

Since the atmospheric drag is the least predictable factor among the forces acting on the LEO satellite, it makes the LEO orbits less predictable, which means that the atmospheric drag coefficient needs to be updated more frequently for accurate OD. Thus, this study will continue to further investigate the accuracy of the real-time obit prediction as a function of the number of drag coefficients estimated. Unfortunately, only two revolutions of data were tested here, which may not be sufficient to evaluate the validity of the parameters estimation and the effects of each modeling choice (*i.e.*, the varying number of C_D coefficients estimated). Therefore, the arc length of the orbit should be extended to 24 hours to continue this investigation. While empirical force modeling can enhance orbit quality significantly, it is known that these once-per-revolution and/or twice-per-revolution parameters can absorb the gravity information (Zhu, 2004). Therefore, it should be investigated carefully whether this approach can be applied to gravity recovery.

The K_p index, which describes the level of geomagnetic activity, reached 4+ on February 15, 2003, whose data is analyzed herein, indicates moderate geomagnetic activity.

In order to arrive at more conclusive findings related to the number of drag coefficients needed in the LEO OD procedure, future study will be focused on a geomagnetically disturbed period, such as, for example, the strongest geomagnetic storm ever recorded of October 29, 2003 (the K_p index reached 9o, *i.e.*, the highest possible value). In contrast, a quiet geomagnetic day, such as October 11, 2003 (K_p index of 1o, *i.e.*, very low value), will be studied to determine the difference in the effect of drag coefficient modeling as a function of the increased atmospheric densities resulting from geomagnetically disturbed conditions.

REFERENCES

Bae, T., J. Kwon and D. Grejner-Brzezinska (2002): Data Screening and Quality Analysis for Kinematic Orbit Determination of CHAMP Satellite, Proceedings of ION National Technical Meeting, January 28-30, San Diego, California, CD-ROM.

Bock, H. (2003): Efficient Methods for Determining Precise Orbits of Low Earth Orbiters Using the Global Positioning System, Geodätisch-geophysikalische Arbeiten in der Schweiz, Volume 65, Schweizerischen Geodätischen Kommission, Institut für Geodäsie und Photogrammetrie, Eidg. Technische Hochschule Zürich.

Byun, S.H. (2003): Satellite orbit determination using triple-differenced GPS carrier phase in pure kinematic mode, Journal of Geodesy 76: 569-585.

Grejner-Brzezinska, D.A. (1995): Analysis of GPS Data Processing Techniques: In Search of Optimized Strategy of Orbit and Earth Rotation Parameter Recovery, Report No. 432, Department of Geodetic Science and Surveying, The Ohio State University, Columbus, Ohio.

Hedin, A.E. (1991): Extension of the MSIS thermosphere model into the middle and lower atmosphere, Journal of Geophysical Research, 96(A2), 1159-1172.

Hofmann-Wellenhof, B., H. Lichtenegger and J. Collins (1997): *Global Positioning System: Theory and Practice*, 4th edition, Springer-Verlag Wien New York.

Hugentobler, U., S. Schaer and P. Fridez (eds.) (2001): Bernese GPS Software Version 4.2, Astronomical Institute University of Berne.

Kang, Z., S. Bettadpur, B. Tapley and J. Ries (2003): Determination of CHAMP Accelerometer Calibration Parameters. In *First CHAMP Mission Results for Gravity, Magnetic and Atmospheric Studies*, Reigber, Lühr and Schwintzer (eds.), pp. 19-25, Springer-Verlag Berlin Heidelberg 2003.

König, R. and K.H. Neumayer (2003): Thermospheric events in CHAMP Precise Orbit Determination. In *First CHAMP Mission Results for Gravity, Magnetic and Atmospheric Studies*, Reigber, Lühr and Schwintzer (eds.), pp. 112-119, Springer-Verlag Berlin Heidelberg 2003.

Kwon, J.H., Dorota Grejner-Brzezinska, Tae-Suk Bae and Chang-Ki Hong (2003): A Triple Difference Approach to Low Earth Orbiter Precision Orbit Determination, The Journal of Navigation, 56, 457-473.

Montenbruck, O. and E. Gill (2001): *Satellite Orbits: Models, Methods, Applications*, Springer-Verlag Berlin Heidelberg 2000.

MSIS (2004): MSIS homepage, Available at: http://uap-www.nrl.navy.mil/models_web/msis/msis_home.htm, accessed August.

Rubincam, D.P. (1990): Drag on the LAGEOS Satellite, Journal of Geophysical Research, 95(B4), 4881-4886.

Zhu, S., Ch. Reigber and R. König (2004): Integrated adjustment of CHAMP, GRACE, and GPS data, Journal of Geodesy 78: 103-108.